CORRESPONDENCE   OPEN

Tunneling nanotubes between bone marrow stromal cells support transmitophagy and resistance to apoptosis in myeloma

Multiple myeloma (MM) flourishes within the bone marrow (BM), a metabolically unique microenvironment with pronounced spatial oxygen-glucose gradients [1].

Hypoxia and glucose deprivation drive metabolic reprogramming in MM cells [2], reducing mitochondrial activity [3] while enhancing their reliance on glycolysis via the Warburg effect. This metabolic shift fuels rapid ATP production and lactate buildup, creating an acidic niche that supports cancer progression. Targeting oxidative phosphorylation and glycolysis pathways may overcome the disease evolution, inhibiting tumor growth in critical ecosystems [4, 5].

Consistently, it is known that a cell can transfer functional or non-functional mitochondria to other cells, contributing to mitochondrial quality control, thereby sustaining cellular plasticity [6–8]. Intercellular mitochondrial transfer in MM, supporting malignant cell survival, was previously investigated in normoxic co-culture systems, where the transfer of healthy mitochondria from BM stromal cells (BMSCs) to MM cells was observed [9, 10].

However, intercellular mitochondrial dynamics occurring under nutrient starvation and hypoxic conditions mimicking the MM microenvironment remain unexplored.

Here, we set up a new co-culture system mirroring the MM niche by co-culturing MM cells and BMSCs in a hypoxic and glucose-serum-deprived environment (0.2% O_2; OGD), identifying a new mechanism involved in the survival of MM cells.

We found that MM cell survival is sustained by the transcellular degradation of unfunctional mitochondria, or transmitophagy [11], that are transferred from MM cells to BMSCs, along with an intercellular transfer of MM cells mitochondria in post-fission state between BMSCs via Tunneling Nanotubes (TNTs). Notably, when TNTs between BMSCs are destroyed, BMSCs fail to support MM survival in OGD, highlighting the pivotal role of homotypic TNTs between BMSCs for MM progression.

JJN3 MM human cell line and BMSCs were cultured under normoxic control conditions (Nx) or in OGD. Mitochondrial membrane potential (ΔΨ), apoptosis, and TNTs were analyzed (Fig. 1A). The ΔΨ of JJN3 cells was higher compared to that measured for BMSCs, and under OGD conditions, the ΔΨ of JJN3 cells strongly decreased, while the ΔΨ of BMSCs remained unaffected (Fig. 1B). To mimic the hypoxic MM microenvironment, JJN3 cells were co-cultured with BMSCs under both normoxic and OGD conditions, and apoptotic cells were measured. We found that OGD did not affect BMSC survival, and BMSCs were able to rescue JJN3 cells from OGD-induced apoptosis (Fig. 1C). Nx and OGD co-cultures were stained for

F-actin and specifically analyzed for TNTs [12]. It was found that OGD triggers homotypic TNT formation between BMSCs (Fig. 1D), while heterotypic TNTs between JJN3 cells and BMSCs were extremely rare. These homotypic TNTs were observed to be detached from the substrate (Fig. 1E), capable of transferring cargo between BMSCs, and were highly dynamic (Fig. 1F; Supplementary Videos 1 and 2).

To trace the intercellular dynamics of JJN3 mitochondria, JJN3 cells were stained for mitochondria using the fixable Mitotracker Deep Red (JJN3 Mito), washed extensively overnight to ensure removal of excess dye, and co-cultured with BMSCs under Nx or OGD conditions. The cells were then analyzed by confocal microscopy to determine JJN3 mitochondrial localization (Fig. 2A). Confocal microscopy revealed the presence of JJN3 mitochondria inside BMSCs. Under OGD conditions, the intercellular transfer of mitochondria increased, and the size of the transferred mitochondria was smaller compared to Nx, indicating that OGD triggers the transfer of mitochondria from JJN3 cells to BMSCs and that in OGD JJN3 mitochondria inside BMSCs were in a post-fission state (Fig. 2B). Transwell-based co-culture experiments showed no passive dye diffusion (Supplementary Fig. 1). Analysis of gap junction protein Connexin 43 (CX43) localization revealed that JJN3 cells were in direct contact with BMSCs via CX43 junctions, and JJN3 mitochondria appeared to be internalized by BMSCs through these CX43 junctions (Fig. 2C), suggesting a CX43-dependent intercellular mitochondrial transfer [7]. Heterotypic TNTs between JJN3 cells and BMSCs were extremely rare, and no mitochondria were found inside them.

We further analyzed the co-culture for lysosomal-associated membrane protein 1 (Lamp1). Confocal microscopy clearly showed JJN3 mitochondria inside BMSCs interacting with Lamp1, with enhanced colocalization under OGD conditions. A more detailed analysis of JJN3 mitochondrial and Lamp1 localization and morphology in BMSCs revealed that, under OGD conditions, large masses of JJN3 mitochondria appeared to be internalized by BMSCs within an actin cage, surrounded by Lamp1, which is typical of damaged mitochondria destined for mitophagy [13] (Fig. 2D, central panel).

Once inside BMSCs, multiple mitochondria-Lamp1 contacts were observed, and fission points were identified in JJN3 mitochondria (Fig. 2D, bottom panel, white arrows). Notably, lysosomal contacts mark the sites of mitochondrial fission [14]. Since JJN3 mitochondria lose membrane potential under OGD, a well-known trigger for mitophagy [15], and various signs of fission appear in BMSCs for JJN3 mitochondria, we conclude that JJN3-to-BMSCs transmitophagy [11, 13] occurs under OGD conditions.

We analyzed TNTs between BMSCs under OGD conditions for the presence of JJN3 mitochondria and Lamp1 localization. The
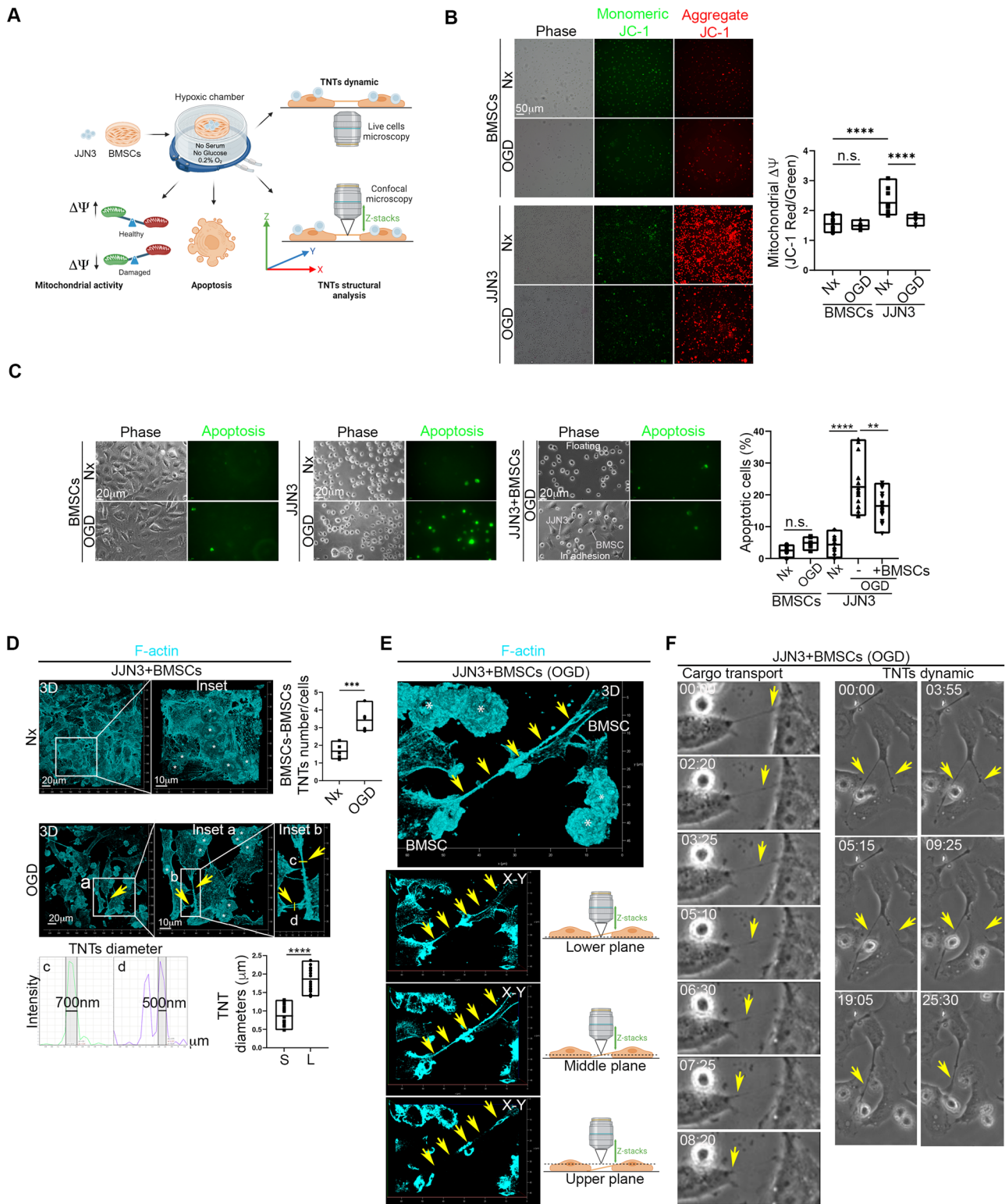
Fig. 1 BMSCs rescue JJN3 from OGD-induced and mitochondrial-dependent apoptosis and generate an extensive homotypic TNTs intercellular network. A Schematic representation of the Oxygen-Glucose Deprivation (OGD) co-culture model used here. JJN3 cells were co-cultured with BMSCs under normoxic control conditions (Nx) or in the absence of serum, glucose, and in a hypoxic environment ($0.2\%O_2$; OGD). The co-culture was analyzed for mitochondrial membrane potential ($\Delta\Psi$), cell apoptosis, TNT structure (confocal microscopy), and TNT dynamics (live-cell microscopy). **B** OGD strongly affects mitochondrial membrane potential (measured through JC-1; $\Delta\Psi$) in JJN3 cells, while BMSCs preserve $\Delta\Psi$ under OGD conditions. ****$p < 0.0001$. **C** JJN3 cells become apoptotic under OGD, while BMSCs are largely unaffected. When co-cultured with JJN3 cells, BMSCs rescue JJN3 cells from OGD-triggered apoptosis. ****$p < 0.0001$; **$p = 0.0068$. **D–F**. OGD induces the formation of homotypic tunneling nanotubes (TNTs) between BMSCs cells (Nx vs OGD ***$p = 0.002$). The diameters of small (S) and large (L) TNTs were measured (full width at half maximum, FWHM. ****$p < 0.001$) (**D**). These TNTs were found to be detached from the surface (**E**) and transported cargo between BMSCs cells (**F**; Supplementary Video 1–2). In (**D**) and (**E**), asterisks indicate JJN3 cells.

Figure panels A–I
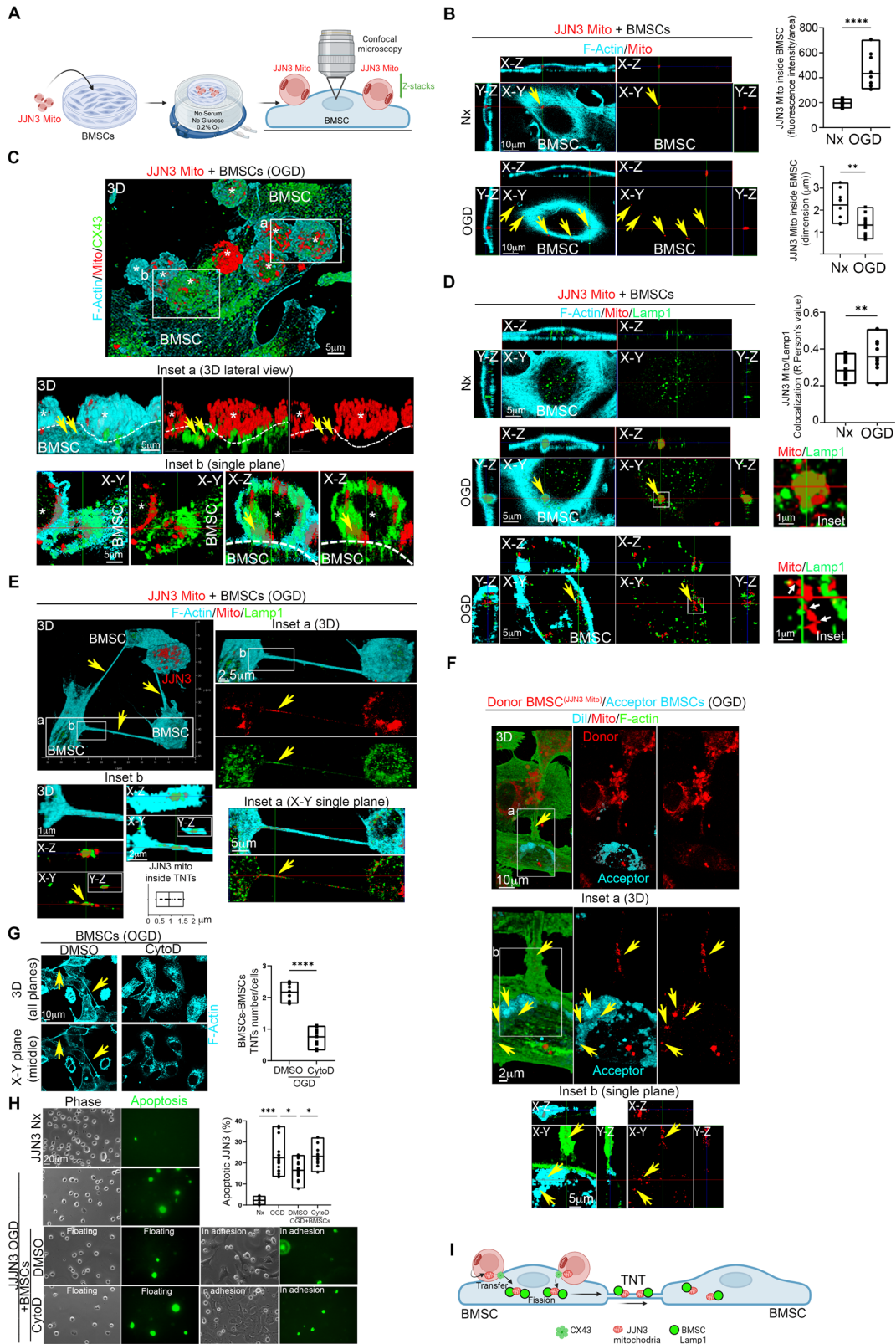
analysis revealed that the homotypic TNTs network between BMSCs contains small JJN3 mitochondria in a post-fission state, along with Lamp1 (Fig. 2E, inset a), and punctate JJN3 mitochondria interacting with Lamp1 (Fig. 2E, inset b).

To assess whether TNTs between BMSCs can transfer these mitochondria between BMSCs, we co-cultured BMSCs with JJN3 mitochondria under OGD for 24 h and washed out JJN3 cells, generating donor BMSCs$^{(JJN3\ Mito)}$. Subsequently, donor

4

Fig. 2 **TNTs between BMSCs transfer JJN3 mitochondria in post-fission state and contribute to JJN3 resistance to OGD. A** Schematic representation of the co-culture model used here. Mitochondria of JJN3 cells were stained with fixable Mitotracker Deep Red and co-cultured under normoxic (Nx) or OGD conditions with BMSCs. The co-culture was analyzed for mitochondrial transfer and colocalization with Lamp1 in BMSCs through confocal microscopy. **B** Quantification of mitochondrial transfer from JJN3 cells to BMSCs under Nx and OGD conditions. OGD triggers intercellular mitochondrial transfer for small post-fission mitochondria. ****$p < 0.0001$; **$p = 0.0082$. **C** JJN3 cells interact with BMSCs through CX43. Confocal microscopy of the OGD co-culture shows high CX43 abundance in the interaction region, and mitochondria frequently colocalize with CX43. **D** OGD triggers the colocalization of JJN3 mitochondria and Lamp1 in BMSCs. Note the presence of an actin cage typical of damaged mitochondria destined for mitophagy (central panel). Once inside BMSCs, multiple fission points were observed in JJN3 mitochondria (bottom panel, white arrows). **$p = 0.0079$. **E** TNTs between BMSCs in co-culture with JJN3 Mito under OGD conditions contain lysosomes and small JJN3 mitochondria in post-fission state. The co-culture was analyzed using high-resolution confocal microscopy for F-actin (cyan), JJN3 mitochondria (red), and Lamp1 (green). Note the presence of small mitochondria, with an average size of $1 \pm 0.5 \mu m$, originating from JJN3 cells inside TNTs between BMSCs. Lamp1 frequently co-localizes with JJN3 mitochondria inside the TNTs. **F** TNTs between BMSCs can transfer small JJN3 mitochondria in a post-fission state from one BMSC to another. A co-culture in OGD conditions, composed of donor BMSC (JJN3 Mito) (red) and acceptor BMSCs stained with DiI (Cyan), shows F-actin-positive (green) TNTs connecting donor and acceptor BMSCs (inset a) and the presence of JJN3 mitochondria inside the acceptor BMSCs (inset a). **G** Cytochalasin-D (CytoD) in OGD destroys TNTs between BMSCs. ****$p < 0.0001$. **H** TNTs between BMSCs contribute to JJN3 apoptotic resistance in OGD. Analysis of caspase 3/7 activity (green) reveals that pre-treatment of BMSC with CytoD prevents the rescue of JJN3 cells in OGD conditions. ***$p = 0.0003$; *$p = 0.04$ (OGD vs OGD+BMSCs); *$p = 0.015$ (OGD+BMSCs+DMSO vs OGD+BMSCs+CytoD). **I** Model of TNTs-mediated BMSCs-to-BMSCs JJN3 mitochondrial transfer supporting JJN3-to-BMSCs transmitophagy.
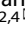
BMSCs$^{(JJN3\ Mito)}$ were incubated with acceptor BMSCs stained with DiI under OGD conditions. We found that donor BMSCs$^{(JJN3\ Mito)}$ were connected to acceptor BMSCs via TNTs containing JJN3 mitochondria in a post-fission state and these mitochondria localize in acceptor BMSCs. These findings demonstrate that TNTs between BMSCs can transfer small JJN3 mitochondria in a post-fission state between BMSCs (Fig. 2F).

To test whether TNTs between BMSCs play a functional role in protecting JJN3 cells from OGD-triggered apoptosis, we disrupted the TNTs network between BMSCs in OGD using 0.5 μM Cytochalasin-D (CytoD) for 24 h. At this concentration and incubation time, this drug disrupts TNTs between BMSCs while preserving BMSCs viability (Supplementary Fig. 2). After washing out CytoD, we co-cultured CytoD pre-treated BMSCs with JJN3 cells under OGD conditions. Analysis of TNTs and cell apoptosis revealed that pre-treatment with CytoD destroys the TNTs network between BMSCs (Fig. 2G) and prevents the rescue of JJN3 cells from OGD-triggered apoptosis (Fig. 2H). Taken together, our data show that the TNTs network between BMSCs allows the intercellular transfer of post-fission JJN3 mitochondria, supporting JJN3-to-BMSCs transmitophagy and contributing to the survival of JJN3 cells in the hypoxic MM niche (Fig. 2I).

Our findings uncover a crucial metabolic adaptation in MM: we show that in a co-culture system mimicking the hypoxic MM milieu, the ΔΨ of MM cells is strongly affected and, most interestingly, these mitochondria are transferred to BMSCs for fission (transmitophagy). This mechanism has primarily been described in the central nervous system and has not been shown before in cancer [11]. Furthermore, in this context, BMSCs support MM cell survival by generating an active.

TNTs network among themselves for the transfer of MM mitochondria in a post-fission state, facilitating efficient transmitophagy within the BMSCs population. To the best of our knowledge, this is the first evidence of a concerting role for transmitophagy and a TNTs network in the OGD MM microenvironment. Undeniably, treatments targeting oxidative phosphorylation, such as proteasome inhibitors are known to induce endoplasmic reticulum stress and apoptosis in MM cells. Hence, resistance mechanisms driven by mitochondrial adaptations highlight the importance of metabolic plasticity. The quiescent MM cells, which are resistant to standard and novel agents, could correlate with metabolic shift sustaining the minimal residual disease in OGD [16].

Overall, preventing TNTs-mediated intercellular mitochondrial exchange could weaken the protective environment that BMSCs provide to MM cells. This could represent a new frontier in MM therapy focused on metabolic vulnerabilities.

Antonio Giovanni Solimando (ID)^{1,5}, Francesco Di Palma (ID)^{2,5}, Vanessa Desantis (ID)^{3}, Angelo Vacca (ID)^{1}, Maria Svelto (ID)^{2} and Francesco Pisani (ID)$^{2,4 \boxtimes}$

^{1}Department of Precision and Regenerative Medicine and Ionian Area (DiMePRe-J), Unit of Internal Medicine "Guido Baccelli", University of Bari "Aldo Moro" Medical School, Bari, Italy. ^{2}Department of Biosciences, Biotechnologies and Environment, University of Bari "Aldo Moro", Bari, Italy. ^{3}Department of Precision and Regenerative Medicine and Ionian Area (DiMePRe-J), Section of Pharmacology, University of Bari "Aldo Moro" Medical School, Bari, Italy. ^{4}Center for Synaptic Neuroscience and Technology, Istituto Italiano di Tecnologia, Genova, Italy. ^{5}These authors contributed equally: Antonio Giovanni Solimando, Francesco Di Palma. $^{\boxtimes}$email: francesco.pisani@uniba.it

DATA AVAILABILITY
Data used for analysis can be made available upon reasonable request.

REFERENCES

1. Hu J, Van Valckenborgh E, Menu E, De Bruyne E, Vanderkerken K. Understanding the hypoxic niche of multiple myeloma: therapeutic implications and contributions of mouse models. Dis Model Mech. 2012;5:763–71.
2. Wu S, Kuang H, Ke J, Pi M, Yang D-H. Metabolic reprogramming induces immune cell dysfunction in the tumor microenvironment of multiple myeloma. Front Oncol. 2020;10:591342.
3. Fujiwara S, Wada N, Kawano Y, Okuno Y, Kikukawa Y, Endo S, et al. Lactate, a putative survival factor for myeloma cells, is incorporated by myeloma cells through monocarboxylate transporters 1. Exp Hematol Oncol. 2015;4:12.
4. Rizzieri D, Paul B, Kang Y. Metabolic alterations and the potential for targeting metabolic pathways in the treatment of multiple myeloma. J Cancer Metastasis Treat. 2019;5:26.
5. Torcasio R, Gallo Cantafio ME, Veneziano C, De Marco C, Ganino L, Valentino I, et al. Targeting of mitochondrial fission through natural flavanones elicits anti-myeloma activity. J Transl Med. 2024;22:208.
6. Li H, Sun W, Gong W, Han Y. Transfer and fates of damaged mitochondria: role in health and disease. FEBS J. 2024. https://doi.org/10.1111/febs.17119.
7. Borcherding N, Brestoff JR. The power and potential of mitochondria transfer. Nature. 2023;623:283–91.
8. Liu H, Mao H, Ouyang X, Lu R, Li L. Intercellular mitochondrial transfer: the novel therapeutic mechanism for diseases. Traffic. 2024;25:e12951.
9. Marlein CR, Piddock RE, Mistry JJ, Zaitseva L, Hellmich C, Horton RH, et al. CD38-driven mitochondrial trafficking promotes bioenergetic plasticity in multiple myeloma. Cancer Res. 2019;79:2285–97.
10. Matula Z, Mikala G, Lukácsi S, Matkó J, Kovács T, Monostori É, et al. Stromal cells serve drug resistance for multiple myeloma via mitochondrial transfer: a study on primary myeloma and stromal cells. Cancers. 2021;13:3461.
11. Davis CO, Kim K-Y, Bushong EA, Mills EA, Boassa D, Shih T, et al. Transcellular degradation of axonal mitochondria. Proc Natl Acad Sci USA. 2014;111:9633–8.

12. Sáenz-de-Santa-María I, Henderson JM, Pepe A, Zurzolo C. Identification and characterization of tunneling nanotubes for intercellular trafficking. Curr Protoc. 2023;3:e939.
13. Kruppa AJ, Buss F. Actin cages isolate damaged mitochondria during mitophagy. Autophagy. 2018;14:1644–5.
14. Wong YC, Ysselstein D, Krainc D. Mitochondria-lysosome contacts regulate mitochondrial fission via RAB7 GTP hydrolysis. Nature. 2018;554:382–6.
15. Harper JW, Ordureau A, Heo J-M. Building and decoding ubiquitin chains for mitophagy. Nat Rev Mol Cell Biol. 2018;19:93–108.
16. Besse L, Besse A, Mendez-Lopez M, Vasickova K, Sedlackova M, Vanhara P, et al. A metabolic switch in proteasome inhibitor-resistant multiple myeloma ensures higher mitochondrial metabolism, protein folding and sphingomyelin synthesis. Haematologica. 2019;104:e415–9.

ACKNOWLEDGEMENTS

AUTHOR CONTRIBUTIONS

All authors contributed to the preparation of this manuscript, approved the final submitted version, and agreed to be listed as authors. FP and AGS designed the research; FDP, VD, FP, and AGS performed the experiments; all authors participated in the analysis and interpretation of the data. AGS, FP, FDP, and VD wrote the manuscript. FP, AV, and MS supervised the research and revised the manuscript. AGS obtained informed consent and primary samples. FP, MS and AGS provided financial support for the research.

COMPETING INTERESTS

AGS has received speaker honoraria from Sanofi, Amgen, and AstraZeneca. He has also participated in advisory boards for Pfizer and Menarini and received travel support for educational purposes from Janssen-Cilag. AV received speaker honoraria from Pfizer, Sanofi, Bristol Myers Squibb, Takeda, Janssen-Cilag, AstraZeneca, Menarini, and Amgen. Their potential conflicts of interest do not imply bias or influence on the authors' opinions or actions. The authors recognize the importance of transparency in the scientific field and are committed to upholding their integrity and maintaining trust in them within the scientific community.

ETHICS APPROVAL

This study was conducted following the Declaration of Helsinki, the Council for International Organizations of Medical Sciences (CIOMS) International Ethical Guidelines, applicable International Council for Harmonization of Technical Requirements for Pharmaceuticals for Human Use (ICH-GCP) Good Clinical Practice guidelines, and applicable local laws and regulations. The study protocol was reviewed and approved by Institutional Review Boards and an Independent Ethics Committee (Resolution No. 1300, dated 12/21/2023). All subjects involved provided signed informed consent.

ADDITIONAL INFORMATION

Supplementary information The online version contains supplementary material available at https://doi.org/10.1038/s41408-025-01210-2.

Correspondence and requests for materials should be addressed to Francesco Pisani.

Reprints and permission information is available at http://www.nature.com/reprints

Publisher's note Springer Nature remains neutral with regard to jurisdictional claims in published maps and institutional affiliations.